Electrochemical Corrosion Properties of $Ti_{46}Zr_{20}V_{12}Cu_5Be_{17}$ In Situ Metallic Glass Matrix Composites in HCl Solutions

Fan Yang

Abstract The electrochemical corrosion properties of in situ $Ti_{46}Zr_{20}V_{12}Cu_5Be_{17}$ metallic glass matrix composites (MGMCs) in HCl solutions have been investigated. The EDS results show that the decrease of protection properties of passive film is caused by reduction of element content of Ti and Zr in passive film, leading to the acceleration of corrosion rate with the increase in of HCl solution concentration. The SEM results indicate that a galvanic effect between matrix and crystalline results in prior dissolution of matrix. With the increasing of Cl ion concentration, the corrosion-induced damage on sample surface augments and crystalline dendrites are completely revealed.

1 Introduction

Bulk metallic glasses (BMGs) produced huge interests and extensive attention in scientific research fields in recent years, because of its high strength, high hardness, excellent soft magnetic properties, and high corrosion resistance [1, 2]. However, the engineering application of BMGs was hindered because of their brittle fracture behavior [3–5]. To circumvent the poor damage tolerance of BMGs, so-called dendrite-reinforced metallic glass matrix composites have been exploited, such as a series of materials named as in situ metallic glass matrix composites (MGMCs) [6, 7]. This achievement was considered as a breakthrough because room temperature plastic deformation improvement was achieved from these MGMCs materials. However, as a excellent performance and wide application prospect material, researchers are less concerned about its electrochemical corrosion properties. There are only a few reports on this aspect about this materials previously. Previous studies on corrosion properties of BMGs have focused on single amorphous materials. Debnath et al. [8, 9] investigated the corrosion behaviors of Ti-based in situ MGMCs. They found that the introduction of the second phase had a major impact on the corrosion properties of this material, which was ascribed to the preferential dissolution

F. Yang (✉)
Beijing Beiye Functional Materials Corporation, Haidian District, Beijing 100192, China
e-mail: clh19610714@163.com

Y. Han (ed.), *Physics and Engineering of Metallic Materials*, Springer Proceedings in Physics 217, https://doi.org/10.1007/978-981-13-5944-6_67

by a galvanic effect in matrix compared to crystalline because of different corrosion resistances between different structure and composition.

The electrochemical properties of $Ti_{46}Zr_{20}V_{12}Cu_5Be_{17}$ in situ MGMCs with mechanical excellent properties were researched [10], containing β-phase (bcc) and conduct the electrochemical corrosion tests on these samples in different HCl solutions. For researching the mechanism of corrosion behavior, the analysis of constitution and microstructure after electrochemical test were conducted.

2 Experiment

The alloys of ingots with nominal composition of $Ti_{46}Zr_{20}V_{12}Cu_5Be_{17}$ were cast into Φ3 mm rods by using a copper mold. The microstructure of alloys was obtained by using X-ray diffractometry (XRD) and scanning electron microscope (SEM) coupled with energy-dispersive X-ray (EDS). Before the electrochemical corrosion test, for the purpose to samples surface clean, the samples were polished with 2500 grit SiC paper and ultrasonically cleaned. All electrochemical tests were conducted in different concentration HCl solutions, respectively. Testing system is a three-electrode cell setup, with a $Hg/HgSO_4$ (K_2SO_4) reference electrode and platinum as counter electrode. Testing system about CHI660E was employed to conduct measurements. The scan rate of dynamic potential polarization test is 1 mV/s, and the test range is −1.0 to 1.5 V. Before test, to ensure open-circuit potential, the samples were immersed in solution for about 1 h. The corrosion current density (i_{corr}) values were calculated by Tafel slope method. Each electrochemical measurement was tested at least three times for repeatability in order to ensure the test data is stable.

3 Results and Discussion

3.1 Structure Characterization

Figure 1a presents a typical XRD pattern obtained from these MGMCs ingots. Figure 1b is SEM images of cross section surface of rod. The presence of body-centered cubic (bcc) β-Ti solid solution can be observed by the diffraction peak.

3.2 Electrochemical Corrosion Measurements

Figure 2 shows potentiodynamic polarization curves for $Ti_{46}Zr_{20}V_{12}Cu_5Be_{17}$ in situ MGMCs rods in different HCl solutions. As can be seen from Fig. 2, the samples have a similar corrosion tendency in different solutions through the pattern. However,

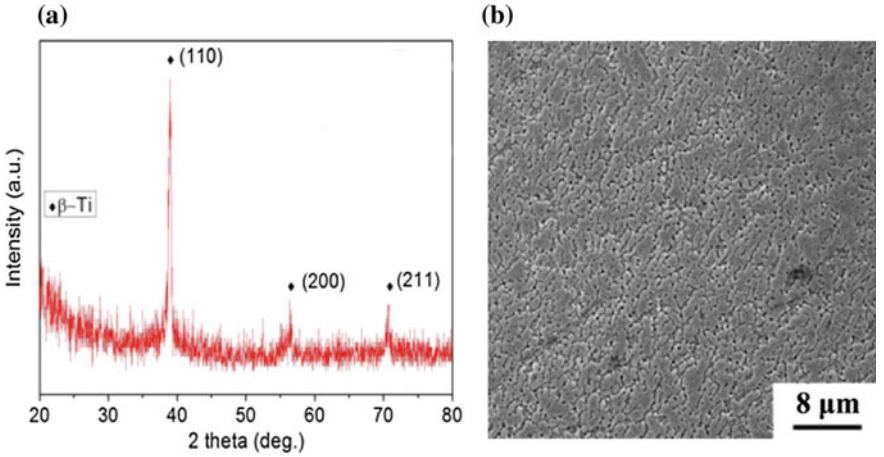

Fig. 1 **a** XRD spectra for as-cast Φ3 mm $Ti_{46}Zr_{20}V_{12}Cu_5Be_{17}$ composites rods; **b** SEM images of cross section surface of rod

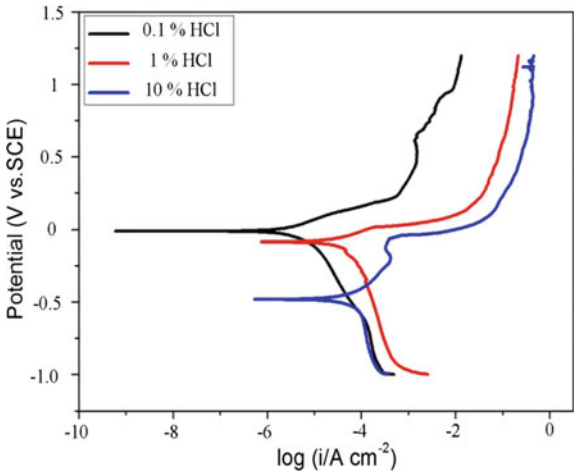

Fig. 2 The potentiodynamic polarization curves of samples in HCl solution of different concentrations

the sample in different solutions have different values of i_{corr}, E_{corr}, and i_{pass}. The test data are listed in Table 1. The values of i_{corr} for sample in 0.1% HCl solution are the lowest, while samples in 10% HCl solution possess the highest values, in addition, for sample in 0.1% HCl solution, the value of E_{corr} is the highest among all the samples, and the value of i_{pass} is the lowest among all the samples, suggesting that sample in 0.1% HCl solutions shows the best corrosion resistance. As the concentration of solutions increases, the corrosion of materials gradually deteriorates.

Figure 3 shows the results of EIS about $Ti_{46}Zr_{20}V_{12}Cu_5Be_{17}$ in situ MGMCs rods in different HCl solutions. The equivalent circuit was shown in the inset of Fig. 3. The radius of capacitance arc implying much more dense passivation layer formed

Table 1 Calculated corrosion parameters of all alloys

Solutions	E (V vs. $Hg/HgSO_4$)	i_{corr} ($\times 10^{-6}$ A/cm^2)
0.1% HCl	-0.01 ± 0.01	3.28 ± 1.13
1% HCl	-0.12 ± 0.03	72.8 ± 10.4
10% HCl	-0.49 ± 0.15	82.8 ± 12.5

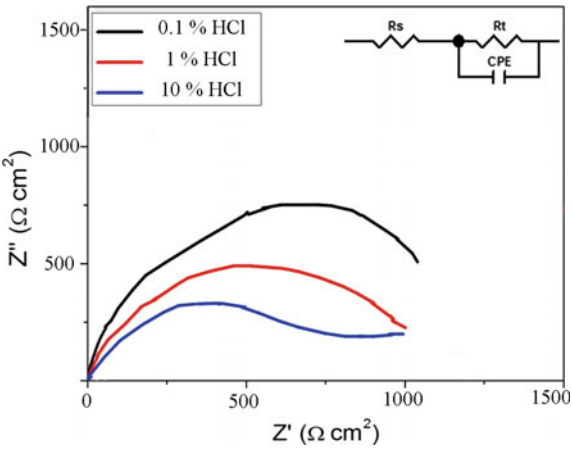

Fig. 3 Nyquist plots of Φ3 mm $Ti_{46}Zr_{20}V_{12}Cu_5Be_{17}$ composites rods in HCl solution of different concentrations. Inset of the corresponding equivalent circuit

on the surface after electrochemical test in 0.1% HCl solution. It is also noteworthy that the result is consistent with the potentiodynamic polarization curves.

3.3 Proposition of Possible Corrosion Mechanism

EDS analysis has been conducted on the samples before electrochemical tests and after electrochemical tests. For in situ MGMCs rods samples in different HCl solutions to shed light on its corrosion mechanisms. Table 2 lists the compositional data obtained by EDS analysis on $Ti_{46}Zr_{20}V_{12}Cu_5Be_{17}$ samples before electrochemical tests and after the electrochemical tests in 0.1 and 10% HCl solutions. Careful inspection of Table 2 shows that the composition of each element after in 0.1% HCl solutions is not much different than before tests, and elemental concentration of Ti and Zr undergoes a considerable variation after electrochemical tests in HCl solutions with concentration changing from 0.1 to 10%. To be brief, in the amorphous matrix, the atomic concentration percentage of Ti exhibits a considerable reduction from 58.5 to 54.7%, while Zr content drops from 21.7 to 18.4%. In crystalline dendrites, Ti content drops from 62 to 55.5%, and Zr content drops from 22.2 to 18.6%. It is believed that this observed elemental content variation is a good indicator of the surface protective layers evolution.

Table 2 The compositional information of alloys after electrochemical tests

Percent (at.%)								
	Crystalline dendrites				Amorphous matrix			
Atomic	Ti	Zr	V	Cu	Ti	Zr	V	Cu
Pretests	62.5	22.4	12.1	2.5	58.6	22.1	12.5	6.8
0.1% HCl	62.0	22.2	13.6	2.2	58.5	21.7	14.3	5.5
10% HCl	55.5	18.6	22.1	2.1	54.7	18.4	23.7	3.2

Since element Ti and Zr are active metals, it will be oxidized in an acidic solution to form a passivation layer, thereby protecting the surface and preventing impurities damaged the alloy surface. Previous studies had shown that the passivation films containing Ti and Zr elements have a strong protective effect on the surface of the material [11–14]. As a logic postulation, the elements Ti and Zr play a crucial role on the formation of protective layers on the surface of in situ MGMCs, and it combines with oxygen to form a metal oxide which is effective against impurities and further destroys the metal surface through the passivation layer. Due to the corrosion environment embrace Cl ion that can damage passive layer, with the increasing of the content of Cl ion, the quality of passive film in surface is not well gradually. Therefore, Ti and Zr content reduction, demonstrated by EDS measurements, strongly suggests that the protective Ti or Zr containing films are diminishing. Another piece of evidence comes from the topographical observation. As displayed in Fig. 4, the corrosion extent induced damage on sample surface augments with the increasing of Cl ion concentrations.

Additionally, the crystalline dendrites can be seen emerging from the surface of the alloys, which indicated that the matrices could have been corroded in the HCl solution. Table 2 indicates that Ti and Zr content decrease in both glass matrix and crystalline dendrite. We assume more Ti and Zr content are beneficial to the passive film formation. By the same token, the relatively more Ti and Zr content in crystalline dendrites might imply that the passive film in crystalline phase has a superior property. Due to the composition and phase discrepancy between the different structure and phase, the glass matrix might serve an anode to the adjacent crystalline dendrites. The preferential dissolution of the amorphous matrix indicates that there is a galvanic between the amorphous matrix and the dendrite due to the difference in composition and structure, and it accelerates breakage of metastable phase [9, 15]. Gebert et al. [15] accredited the similar conclusion about electrochemical corrosion properties of MGMCs.

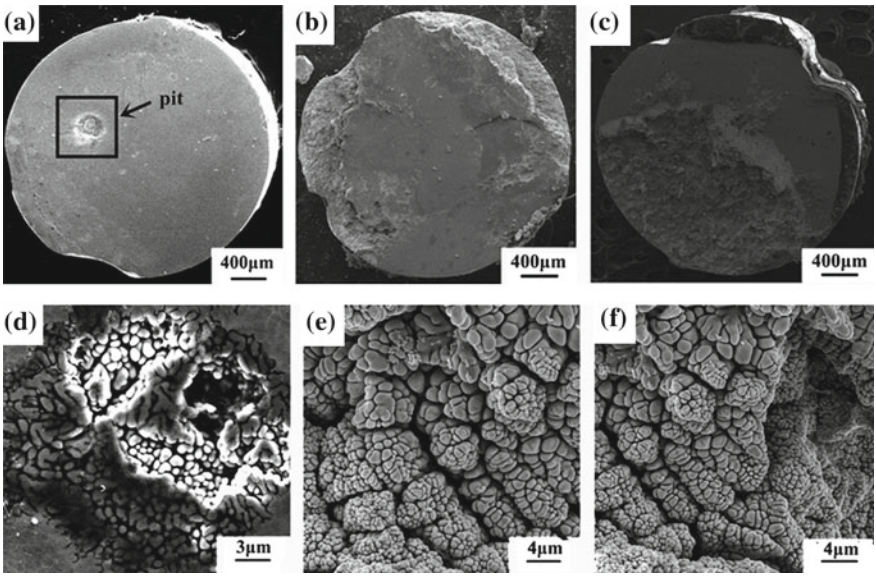

Fig. 4 SEM images of the $Ti_{46}Zr_{20}V_{12}Cu_5Be_{17}$ alloy surface after potentiodynamic polarization test in HCl solutions of different concentrations. The images of sample in 0.1% HCl, with **a** full image, **d** partially magnified image, respectively. The images of sample in 1% HCl, with **b** full image, **e** partially magnified image, respectively. The images of sample in 10% HCl, with **c** full image, **f** partially magnified image, respectively

4 Conclusions

A comprehensive electrochemical performance analysis of in situ $Ti_{46}Zr_{20}V_{12}Cu_5Be_{17}$ metallic glass matrix composites in different HCl solutions was conducted. The decrease of protection properties of passive film is caused by reduction of element content of Ti and Zr in passive film, leading to the acceleration of corrosion rate with the increasing of HCl solution concentration. The composition and phase discrepancy between the different microstructure leads to a galvanic effect which results in the dissolution of the less stable amorphous matrix. With the increasing of Cl ion concentrations, the corrosion-induced damage on sample surface augments and crystalline dendrites completely appear and amorphous matrices almost disappear.

References

1. A. Inoue, Stabilization of metallic supercooled liquid and bulk amorphous. Acta Mater. **48**, 279–306 (2000)

2. C.C. Hays, C.P. Kim, W.L. Johnson, Microstructure controlled shear band pattern formation and enhanced plasticity of bulk metallic glasses containing in situ formed ductile phase dendrite dispersions. Phys. Rev. Lett. **84**, 2901–2904 (2000)
3. D.C. Hofmann, J.Y. Suh, A. Wiest, G. Duan, M.L. Lind, M.D. Demetriou, W.L. Johnson, Development of tough, low density titanium-based bulk metallic glass matrix composites with tensile ductility. Proc. Natl. Acad. Sci. U.S.A. **105**, 20136–20140 (2008)
4. D.C. Hofmann, J.Y. Suh, A. Wiest, G. Duan, M.L. Lind, M.D. Demetriou, W.L. Johnson, Designing metallic glass matrix composites with high toughness and tensile ductility. Nature **451**, 1085–1089 (2008)
5. J.W. Qiao, Y. Zhang, G.L. Chen, Fabrication and mechanical characterization of a series of plastic Zr-based bulk metallic glass matrix composites. Mater. Des. **30**, 3966–3971 (2009)
6. J.W. Qiao, A.C. Sun, E.W. Huang, Y. Zhang, P.K. Liaw, C.P. Chuang, Tensile deformation micromechanisms for bulk metallic glass matrix composites: from work-hardening to softening. Acta Mater. **59**, 4126–4137 (2011)
7. P.F. Gostin, R. Sueptitz, A. Gebert, U. Kuehn, L. Schultz, Comparing the corrosion behaviour of Zr_{66}/Ti_{66}–$Nb_{13}Cu_8Ni_{6.8}Al_{6.2}$ bulk nanostructure-dendrite composite. Intermetallics **16**, 1179–1184 (2008)
8. M.R. Debnath, D.H. Kim, E. Fleury, Dependency of the corrosion properties of in situ Ti-based BMG matrix composites with the volume fraction of crystalline phase. Intermetallics **22**, 255–259 (2012)
9. M.R. Debnath, H.J. Chang Kim, E. Fleury, Effect of group 5 elements on the formation and corrosion behavior of Ti-based BMG matrix composites reinforced by icosahedral quasi crystalline phase. J. Alloy. Compd. **612**, 134–142 (2014)
10. J.W. Qiao, T. Zhang, F.Q. Yang, P.K. Liaw, S. Pauly, B.S. Xu., A tensile deformation model for in situ dendrite/metallic glass matrix composites. Sci. Rep. https://doi.org/10.1038/srep02816
11. C.L. Qin, J.J. Oak, N. Ohtsu, K. Asami, A. Inoue, XPS study on the surface films of a newly designed Ni-free Ti-based bulk metallic glass. Acta Mater. **55**, 2057–2063 (2007)
12. R. Kaufmann, H. Klewe-Nebenius, H. Moers, G. Pfennig, H. Jenett, H. Ache, XPS and AES investigations of the reaction behaviour of iodine with zircaloy-4 surfaces. Surf. Interface Anal. **11**, 502–509 (1998)
13. M.M. Lohrengel, Thin anodic oxide layers on aluminium and other valve metals. Mater. Sci. Eng. **11**, 243–294 (1993)
14. J.R. Birch, T.D. Burleigh, Oxides formed on titanium by polishing, etching, anodizing, or thermal oxidizing. Corrosion **56**, 1233–1241 (2000)
15. A. Gebert, U. Kuehn, S. Baunack, N. Mattern, L. Schultz, Pitting corrosion of zirconium-based bulk glass-matrix composites. Mater. Sci. Eng. A **415**, 242–249 (2006)